TMA4212 - Buckley-Leverett equation

Candidate numbers: 10052, 10041, 10011

Tuesday 10th April, 2018

1 Introduction

We study the Buckley-Leverett equation, which is a conservation equation used to model the flow of two immiscible fluid phases in a porous medium. It describes, for example, the displacement of oil by water in a one-dimensional reservoir. The equation can be derived from the mass conservation equations of incompressible two-phase flow without capillary forces. The equation is on the form

$$u_t + f(u)_x = 0, \tag{1}$$

$$f(u) = \frac{u^2}{u^2 + C(1-u)^2}. \tag{2}$$

Here the constant $C = \mu_w/\mu_n$ describes the ratio between the fluid viscosities. For simplicity we assume $C = 1$. In addition we have initial conditions

$$u(x, 0) = u_0(x). \tag{3}$$

In the course, we have mainly studied finite difference methods, which assume smooth solutions. However, first order quasi-linear hyperbolic equations(conservation laws) will generally give discontinuous solutions even from continuous initial data. We therefore need to find a weak solution, defined as any solution that satisfy the following equation for all smooth and compactly supported test functions ϕ[3]

$$\int\int \left[u\frac{\partial \phi}{\partial t} + f(u)\frac{\partial \phi}{\partial x} \right] dxdt = 0. \tag{4}$$

The analytical solution at time T can be found to be [3]

$$u(x) = \begin{cases} \frac{1}{2}\left(\sqrt{\left(\frac{\frac{-2x}{T} + \sqrt{\frac{4x}{T}+1} - 1}{x/T} + 1 \right)} + 1 \right), & x < \frac{1}{2}(1+\sqrt{2})T, \\ 0, & \text{otherwise.} \end{cases} \tag{5}$$

2 Discretization

As mentioned in the Introduction 1, the discontinuity in our problem motivates us to use finite volume instead of finite difference methods. However, the simplest finite volume methods turn out to be identical to the finite difference methods.

We approximate the solution on a grid, and U_m^n refers to the approximation of $u_m^n = u(x_m, t_n)$ at point $x_m = x_0 + mh$ and time $t_n = t_0 + nk$.

2.1 Classical schemes

To arrive at a discretized equation, we require that (1) holds in an integrated sense. We rewrite it to the integral form

$$\frac{d}{dt}\int_{x_1}^{x_2} u(x,t)dx = f(u(x_1,t)) - f(u(x_2,t)), \tag{6}$$

and define the sliding average as

$$\bar{u}(x,t) = \frac{1}{h}\int_{x-h/2}^{x+h/2} u(\xi,t)dt. \tag{7}$$

We combine (6) and (7) and integrate from t_n to t_{n+1}

$$u_m^{n+1} - u_m^n = \frac{1}{h}\int_{t_n}^{t_{n+1}} f(u(x_{m-1/2},t))dt - \frac{1}{h}\int_{t_n}^{t_{n+1}} f(u(x_{m+1/2},t))dt. \tag{8}$$

Let $F_{m\pm1/2}$ be defined as the flux integral

$$F_{m\pm1/2}^n \approx \frac{1}{h}\int_{t_n}^{t_{n+1}} f(u(x_{m\pm1/2},t))dt, \tag{9}$$

which we approximate by the centered average

$$F_{m\pm1/2}^n = \frac{k}{2}\big[f(U_{m\pm1}^n) + f(U_m^n)\big]. \tag{10}$$

However, the resulting scheme has shown to be unstable. A stable scheme can be obtained by adding a diffution term $\frac{h^2}{k}\partial_x^2 u$ approximated by central differences. This yields the Lax-Friedrich scheme

$$U_m^{n+1} = \frac{1}{2}\big(U_{m+1}^n + U_{m-1}^n\big) - \frac{1}{2}r\big[f(U_{m+1}^n) - f(U_{m-1}^n)\big], \tag{11}$$

where $r = k/h$.

Better accuracy can be achieved by evaluating the flux integrals $F_{m\pm1/2}$ at the midpoints instead of the endpoints. These values can be computed

by using the Lax-Friedrich scheme on a grid with half the grid-spacing. This results in the Lax-Wendroff scheme

$$\begin{aligned} U_{m\pm1/2}^{n+1/2} &= \frac{1}{2}\big(U_m^n - U_{m+1}^n\big) - \frac{1}{2}r\big[f(U_{m\pm1}^n) + f(U_m^n)\big] \\ U_m^{n+1} &= U_m^n - r\big[f(U_{m+1/2}^{n+1/2}) - f(U_{m-1/2}^{n+1/2})\big]. \end{aligned} \tag{12}$$

The methods developed so far use information from both sides of the grid interface when computing approximations to the flux integral (9). However, this is not necessary if we know the structure of the flux function. If we look at (2), we see that for all $0 < u < 1$(which is our domain for u), $f'(u) > 0$. In this way, we know that all characteristics will be positive, so that we only need to use the solution from the left side of the grid interface to evaluate the integral (9). Thus, $F_{m+1/2} = f(u_m^n)$ will be the exact value of the integral, for sufficiently small k, provided that the solution at time t_n is constant and equal to u_m^n in cell m. The resulting scheme is the upwind scheme, and it takes the form

$$U_m^{n+1} = U_m^n - r[f(U_m^n) - f(U_{m-1}^n)], \tag{13}$$

where $r = k/h$ as usual.

When implementing these schemes on a bounded domain, one generally has to modify the stencils in cells next to the boundary to handle boundary conditions. To avoid this, we introduce fictitious nodes at each end of the domain. These nodes are not part of the domain, and their values can be set manually to impose boundary conditions.

2.2 Semi-discrete high-resolution scheme

In Figure 1 we see the results of solving the Buckley-Leverett with the three methods developed in Section 2.1. The Lax-Wendroff method is a second-order method on smooth solutions, but it performs poorly around discontinuities. On the other hand, the Upwind method is only first order, but performs well around discontinuitites. In this section, we introduce another type of discretization that combines the best properties of Lax-Wendroff and Upwind.

The scheme we develop is semi-discrete. If we define $\bar{u}_m(t) = \bar{u}(x_m, t)$ as in equation (7), the evolution of the equation (6) reads

$$\frac{d}{dt}\bar{u}_m(t) = L_m(u(t)) = -\frac{1}{h}\Big[f(u(x_{m+1/2}, t)) - f(u(x_{m-1/2}, t))\Big]. \tag{14}$$

Firstly, we have to get point values at the integration points. Approximate values can be computed from the cell averages $\bar{u}_m(t)$ by applying a piecewise polynomial reconstruction. The simplest approach to get a second order scheme is to apply a linear reconstruction [3, p.304]. We may use forward, backward or central differences. As either of these may overshoot the

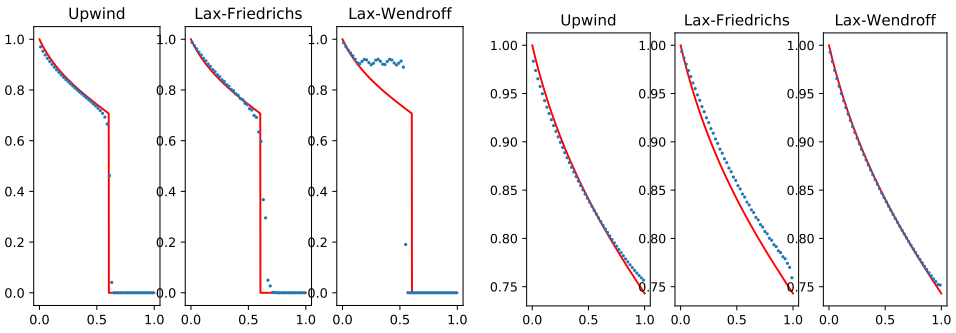

Solution at T = 0.5 Solution at T = 1

Figure 1: Solution of BL equation with $N = 50$ grid points for initial conditions (29)[right] and (30)[left]. The red lines are the analytical solutions, and the blue dots are the solutions obtained by the three different classical methods.

solution at discontinuities, we introduce a nonlinear intelligent agent that combines forward and backward differences or sets it to zero when these have opposite signs.

Reconstruction gives different point values on opposite sides of x_{m+1}. To be able to use the midpoint rule, we need to specify how these one-sided point values should be used to evaluate the integrand. As above, we use upwind flux

$$f(u(x_{m+1/2}, t)) \approx F^{UW}(\bar{u}_m(t), \bar{u}_{m+1}(t)) = f(\bar{u}_m(t)) \tag{15}$$

Finally, we use an explicit TVD Runge-Kutta predictor-corrector scheme to compute the ODE. This family of methods has been developed especially to integrate semi-discrete schemes in time without creating false oscillations [1]. All this results in a second-order method of the form

$$\begin{aligned} U_m^{(1)} &= U_m^n + k[f(u_m^n) - f(u_{m-1}^n)] \\ U_m^{n+1} &= \frac{1}{2}U_m^n + \frac{1}{2}\left[U_m^{(1)} + k(f(U_m^{(1)}) - f(U_{m-1}^{(1)})\right], \end{aligned} \tag{16}$$

This is an example of a second-order high-resolution Godunov scheme. By high-resolution, one means that the scheme has formal high order on smooth solutions but avoids creating oscillations at discontinuities [3].

3 Analysis

3.1 Consistency

First, we prove consistency of the upwind scheme (13). We assume smooth solutions, even though this typically will not be the case. Normally, one

would expect to get a discontinuous solution to the equation. We now go back to finite difference methods, which have the same formulas as the finite volume methods, but the interpretation is different. In addition we assume that the values at the grid points are exact, i.e, $u_m^n = u(x_m, t_n)$. Now, we substitute basic Taylor expansions into the expression for the upwind scheme (13) and denote $u = u_m^n, f = f_m^n$. The truncation error τ_m^n will be

$$\begin{aligned} k\tau_m^n =& u + k\frac{\partial u}{\partial t} + \frac{k^2}{2}\frac{\partial^2 u}{\partial t^2} - u + \frac{k}{h}\left(f - \left(f - h\frac{\partial f}{\partial x} + \frac{h^2}{2}\frac{\partial^2 f}{\partial x^2}\right)\right) \\ &+ O(h^2) + O(k^3) \end{aligned} \tag{17}$$

Hence, we can shorten this expression and find the truncation error

$$\tau_m^n = \frac{k}{2}\frac{\partial^2 u}{\partial t^2} - \frac{h}{2}\frac{\partial^2 f}{\partial x^2} + O(k^2) + O(h^2) \tag{18}$$

The upwind scheme is first order in time and space. It is also consistent, because as $h \to 0, k \to 0$ the truncation error will tend to zero, i.e. $\tau_m^n \to 0$.

Now, we prove consistency of the Lax-Friedrichs scheme (11). Again, as for the upwind scheme, we assume smooth solutions, and that the values at the grid points are exact, i.e. $u_m^n = u(x_m, t_n)$. We substitute Taylor expansions into the Lax-Friedrichs scheme (11) and obtain

$$\begin{aligned} k\tau_m^n =& u + k\frac{\partial u}{\partial t} + \frac{k^2}{2}\frac{\partial^2 u}{\partial t^2} - \frac{1}{2}\left(u + h\frac{\partial u}{\partial x} + \frac{h^2}{2}\frac{\partial^2 u}{\partial x^2} + u - h\frac{\partial u}{\partial x} + \frac{h^2}{2}\frac{\partial^2 u}{\partial x^2}\right) \\ &+ \frac{k}{2h}\left[f + h\frac{\partial f}{\partial x} + \frac{h^2}{2}\frac{\partial^2 f}{\partial x^2} + \frac{h^3}{6}\frac{\partial^3 f}{\partial x^3} - \left(f - h\frac{\partial f}{\partial x} + \frac{h^2}{2}\frac{\partial^2 f}{\partial x^2} - \frac{h^3}{6}\frac{\partial^3 f}{\partial x^3}\right)\right] \\ &+ O(h^3) + O(k^3). \end{aligned} \tag{19}$$

Hence, we can shorten this expression and find the truncation error

$$\tau_m^n = \frac{k}{2}\frac{\partial^2 u}{\partial t^2} - \frac{h^2}{2k}\frac{\partial^2 u}{\partial x^2} + \frac{h^2}{6}\frac{\partial^3 f}{\partial x^3} + O(h^3) + O(k^2). \tag{20}$$

The Lax-Friedrichs is second order in space, but only first order in time. This makes the scheme first order. It is also consistent, because as $h^2 \to 0$, $k \to 0$ the truncation error will tend to zero, i.e. $\tau_m^n \to 0$.

3.2 Stability

We can now go on to prove stability. A finite difference scheme is stable provided that the error at the nodes,

$$e_m^n = |U_m^n - u(x_m, t_n)|$$

does not blow up. If we choose step-sizes that break the interval of absolute stability, the finite difference scheme will become unstable and produce inaccurate results. We use the Fourier method to prove stability of the Upwind scheme. We substitute $u_m^n = \xi^n e^{i\beta mh}$ into the expression to obtain an expression for the amplification factor ξ. Then the scheme is stable when $|\xi| \leq 1$.

Because we assume $f(u)$ to be smooth, we can by the mean value theorem transform the Buckley-Leverett equation (1) into $u_t + au_x = 0$, and look at stability for this equation. Here, $a = f'(\eta)$ for some $\eta \in [u_{m-1}^n, u_m^n]$.

Now, consider the upwind scheme (13), which can be rewritten to (we assume $a > 0$)

$$u_m^{n+1} = u_m^n - ar(u_m^n - u_{m-1}^n), \tag{21}$$

where $r = k/h$. We proceed with the Fourier method

$$\xi^{n+1} e^{i\beta mh} = \xi^n e^{i\beta mh} - ar\xi^n e^{i\beta mh}(1 - e^{-i\beta h}). \tag{22}$$

Dividing by $\xi^n e^{i\beta mh}$ gives

$$\xi = 1 - ar(1 - e^{-i\beta h}) = 1 - ar(1 - \cos\beta h) - iar\sin\beta h, \tag{23}$$

which after some calculations gives us

$$|\xi|^2 = 1 - 4(1 - ar)ar\sin^2\frac{\beta h}{2} \implies ar \leq 1. \tag{24}$$

Thus, for the upwind scheme to be stable, we require $ar \leq 1$. This is the famous CFL-condition.

Now we can go on to prove stability of the Lax-Friedrich scheme in the same way, by substituting $u_m^n = \xi^n e^{i\beta mh}$. This gives

$$\xi^{n+1} e^{i\beta mh} = \frac{1}{2}\xi^n e^{i\beta mh}(e^{i\beta h} + e^{-i\beta h}) - \frac{1}{2}ar\xi^n e^{i\beta mh}(e^{i\beta h} - e^{-i\beta h}). \tag{25}$$

Again, we divide by $\xi^n e^{i\beta mh}$, thus obtaining

$$\xi = \frac{1}{2}(e^{i\beta h} + e^{-i\beta h}) - \frac{1}{2}ar(e^{i\beta h} - e^{-i\beta h}). \tag{26}$$

Now we can utilize Euler's formula, $e^{ix} = \cos x + i\sin x$ to get

$$\xi = \frac{1}{2}(2\cos\beta h) - \frac{1}{2}ar(2i\sin\beta h) = \cos\beta h - iar\sin\beta h. \tag{27}$$

For stability we require $|\xi| \leq 1$, which we see from

$$|\xi|^2 = \cos^2\beta h + (ar)^2\sin^2\beta h, \tag{28}$$

is when $ar \leq 1$, which is the same region as for the upwind scheme.

When conducting numerical experiments on the order of convergence, we cannot look at convergence in time and space separately, because of the

CFL-condition imposing a bound on k for a given h. We compute numerical solutions with decreasing h. To ensure stability, we therefore need $k \leq \frac{h}{|f'(\eta)|}$ owing to the CFL-condition. Because this η is unknown, we set at each iteration

$$k = 0.995 \frac{h}{\max_u |f'(u)|}.$$

4 Numerical verification

We now want to check the accuracy of our code, and verify the results obtained in Section 3. Thus, we create some numerical experiments. We want to check the order of convergence for all the methods on both a smooth and a discontinuous solution. Both experiments have domain $0 < x < 1$. The first experiment computes the solution at time $T = 1$, for initial data

$$u_0(x) = \begin{cases} 1, & x \leq 0, \\ \frac{1}{2}\left(1 + \sqrt{\sqrt{5} - 2}\right), & \text{otherwise}, \end{cases} \tag{29}$$

where $\frac{1}{2}\left(1 + \sqrt{\sqrt{5} - 2}\right)$ is the analytical solution at the endpoint of the domain, $x = 1$ at time $T = 1$ for the solution shown in the right in Figure 1. This creates a solution that is smooth on $0 < x < 1$ at $T = 1$. We compute the numerical solution with the four presented schemes, with number of grid points equal to $M = 2^i$, for $i = 3, \ldots, 10$, giving the results in Figure 2.

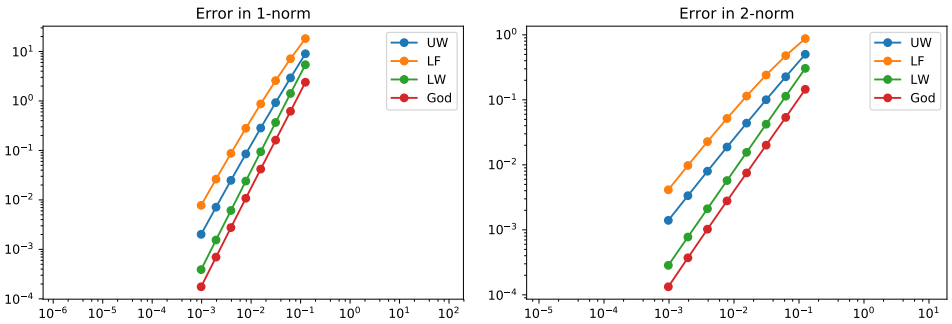

Figure 2: Error plot of the four discretization methods on a continuous problem. The numerically computed solutions are compared to the analytical solution (5).

From this, we see that on a continuous solution, the Lax-Wendroff method has a higher order of convergence than the two other classical schemes, which are of order one. Lax-Wendroff converges with order two on the smooth solution, which is in line with the presented theory. The high-resolution Godunov scheme is also of order two on the smooth solution.

The second experiment we make computes the solution at time $T = 0.5$, for initial data

$$u_0(x) = \begin{cases} 1, & x \leq 0, \\ 0, & \text{otherwise.} \end{cases} \tag{30}$$

which yields the solution on the left in Figure 1, a discontinuous solution. These initial conditions are typical for the Buckley-Leverett equation, and the physical interpretation is that we inject water from the left into an oil-filled reservoir. We compute the numerical solution with grid points as for the first experiment, obtaining the results in Figure 3.

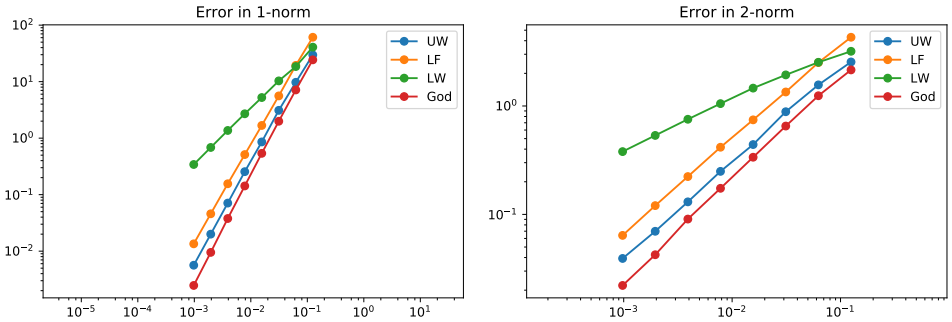

Figure 3: Error plot of the four discretization methods on a discontinuous problem. The numerically computed solutions are compared to the analytical solution (5).

Firstly, we note that the Lax-Wendroff scheme converges very slowly. The Lax-Wendroff scheme will give oscillations around discontinuities because the flux-function is non-convex, and it will not converge to the correct solution. The non-convex flux-function is one of the key differences between the Buckley-Leverett equation and for instance Burger's equation. Furthermore, all the other schemes seem to be of order one. However, the Godunov scheme performs somewhat better. This scheme was designed to be of order two, so we would expect it to perform better than the classical schemes.

When comparing Lax-Friedrichs to Upwind, they have the same slope in both experiments, but upwind is better by a constant number for all h. Even though Lax-Friedrichs is second order in space, it suffers from smearing discontinuities, as seen in Figure 1, and is therefore outperformed by the Upwind scheme.

5 Conclusion

To conclude, we have developed four different schemes for solving the Buckley-Leverett equation. We have analytically showed constistency and order of convergence, as well as stability for two of the schemes. These results were verified numerically, in addition to finding the order of convergence of the two other schemes by conducting experiments on commonly used initial data. Every member of the group contributed equally.

References

[1] S. Gottlieb and C.W. Shu. Total variation diminishing runge-kutta schemes. *Mathematics of Computations*, 67(221):73–85, 1998. http://www.ams.org/journals/mcom/1998-67-221/S0025-5718-98-00913-2/.

[2] J. Hudson. Numerical techniques for conservation laws with source terms, 1998. https://www.reading.ac.uk/web/files/maths/J_Hudson.pdf.

[3] K. A. Lie. *An Introduction to Reservoir Simulation Using MATLAB*. SINTEF ICT, Department of Applied Mathematics, 2017. http://folk.ntnu.no/andreas/mrst/mrst-book.pdf.